LANDING SITE ANALYSIS FOR A LUNAR POLAR WATER ICE GROUND TRUTH MISSION. S. R. Deitrick[1,2], A. T. Russell[2], and S. B. Loza[2] [1]Jacobs/NASA Johnson Space Center, Houston, TX, USA (sarah.r.deitrick@nasa.gov), [2]Center for Space Resources, Colorado School of Mines, Golden, CO, USA (atrussell@mymail.mines.edu, sloza@mymail.mines.edu).

Introduction: Economically viable quantities of water ice are believed to exist at both the north and south poles of the Moon. The small tilt of the Moon (1.5 degrees) results in a very low sun angle at the lunar poles. Because of this, there are places at the poles such as crater interiors that are permanently shadowed by the local topography and do not receive any sunlight. These areas, called Permanently Shadowed Regions (PSRs), can get down to 25 K and act as cold traps to gases that reach their surfaces [1]. Ice has been detected both directly and indirectly within the PSRs at the lunar poles through remote sensing techniques [2] as well as physical results from the Lunar CRater Observation and Sensing Satellite (LCROSS) impact into Cabeus crater at the south pole [3]. These ice deposits are attractive as they can be mined to produce oxygen and hydrogen for propellant as well as water and oxygen for sustaining human life on the lunar surface and in cislunar space. This work proposes landing sites for a ground truth mission at the lunar south pole that will provide answers to these questions to enable science- and prospecting-based exploration. Using the highest resolution remote sensing datasets available, the south pole of the Moon was analyzed to select the best locations that would provide valuable data for water-ice confirmation. This data will then be used to create a model for automated site selection for the Moon.

Crater Selection: Four craters at the south pole of the Moon were selected for landing site analysis: Haworth, Shoemaker, Faustini, and Sverdrup. These are the four largest craters at the south pole, contain the highest concentrations of surface water-ice exposures from [2], have the largest LAMP detections that are consistent with 0.1-2 wt% ice, and have large and relatively flat crater floors that are safe for landing. These craters contain large PSRs that show the most exposures of surface water-ice that are widely distributed, leading to the assumption that they are the PSRs with the highest concentrations of ice with a large spatial distribution. This is not only ideal for ground truth missions, but for prospecting missions and future ISRU (e.g. propellant production) plants as well.

An ideal landing site within these craters will meet the desired requirements of landing within a PSR, maximum summer temperatures of < 110 K, LAMP on band/off band ratio and lyman-α values of 1.2-4 and < 0.03 respectively, slopes < 20°, and roughness values of < 0.4 m.

Landing Site Analysis Methods: The main part of this analysis was conducted using ArcGIS software created by the Environmental Systems Research Institute (ESRI) [4]. The data required for the analysis includes LOLA [5] 5 mpp (down to 87.5°S latitude) and 10 mpp (down to 85°S latitude) DEMs, Diviner polar thermal temperature data [6], LAMP albedo data [7], surface ice exposure location data [2], PSR location data [8], and the LROC [9] 20 mpp NAC long exposure visible imagery of the interiors of PSRs. The open source Geospatial Data Abstraction Library (GDAL) [10] was used to create slope and roughness maps from both LOLA DEMs which were then imported into ArcGIS.

Slope. Candidate landing sites are assessed using a slope criteria of 20 degrees. This ensures that landing modules are not exceeding a 20 degree tilt which could cause issues with instrument performance and prevents the lander from possibly falling on its side. This also ensures terrain traversability for a potential rover.

Roughness. In order for a zone to be considered "safe", the area must be free of boulders larger than 1 m in diameter. Since block distribution data from LRO's Diviner instrument is not available for the lunar south pole, another option to assess boulder and crater distributions on the surface is to use roughness maps which help express the elevation differences between a central pixel and its neighboring eight pixels (a.k.a cells). Roughness is defined as the largest inter-cell difference of a central pixel and its surrounding eight cells. Roughness maps were produced from the 5 mpp and 10 mpp LOLA DEMs. High values represent more rugged and rough terrain (large boulders, steep drop-offs, etc.) whereas low values represent smoother, more level surfaces. Roughness values of 0.4 m (40 cm) and less were used for this site selection to help avoid undesired lander tilt and other safety concerns.

Temperature. The newly released Diviner summer maximum temperature map [6] was used to constrain other datasets to the thermal data. Since there is a very specific cutoff for ice sublimation temperature at < 110 K as defined by [2], the dataset was clipped in ArcGIS to only show temperatures of < 110 K. This allowed for the analysis of areas only within that temperature range. Most of the area within the floors of Haworth, Shoemaker, Faustini, and Sverdrup are all under 110 K.

Lyman-alpha. To analyze water ice abundance, LAMP data from [7] was obtained and modified to show only the values that are representative of specific ice concentrations. The data was imported into the ArcGIS software and the "Extract by Attribute" tool was used to create a query that extracted all on band/off band ratio

values of 1.2 to 4 and all lyman-α values of < 0.03. These values are representative of water ice concentrations of 0.1-2% by mass.

All datasets, including the temperature, slope, roughness, LAMP ice concentration, and surface ice exposure location maps were overlaid on top of each other in order to see which ice exposure locations overlap with all other datasets. This allowed for the simple analysis of determining the safest ice exposure location to land at with a reasonable concentration of water ice for ground truth and future ISRU water ice extraction missions.

Final Site Selection: After analyzing each crater, it was found that Sverdrup crater has several promising locations. The crater has multiple regions of spatially dense ice exposures as shown by the data obtained by [2], with the most promising of these locations shown in Fig. 1. This location has 6 ice exposures located on fairly smooth surfaces (≤ 0.4 m roughness) all constrained by our slope (≤ 20°) and LAMP requirements. Modeling done by [11] has determined the potential depth of the ice in this location as 1 m. The location is not too far from the PSR edge and crater rim (< 5 km) to allow relatively easy access from a crew stationed on the rim.

Future Work: Our next step is to develop a model for automated site selection based on this work. The model will incorporate inputs from all data used thus far as well as additional datasets used in the future. The aim is to have a model that will automatically identify all ideal landing locations based on the desired values of each dataset (e.g. slopes < 20°, roughness < 0.4m, etc.). The results from the model will be compared to our current results to ensure accuracy of our final site selection. Upon completion, this model can be used to identify the safest landing sites with the highest water ice concentrations at the south pole of the Moon. The development of this model will enable science exploration at the lunar south pole both for robotic precursor missions such as CLPS as well as crewed missions to the surface.

Acknowledgments: We gratefully acknowledge the Planetary Data System's Geosciences Node for providing the data used for this research. We would like to thank Shuai Li, Paul Hayne, Robert Mueller, Chris Dreyer, and George Sowers, with whom we had many insightful discussions while writing this paper.

References: [1] Vondrak R. R. and Crider D. H. (2003) *American Scientist, 91,* 322-329. [2] Li S. et al. (2018) *National Academy of Sciences, 115,* 8907-8912. [3] Colaprete A. et al. (2010) *Science, 330,* 463-468. [4] ESRI (2012) *ArcGIS Release 10.1.* [5] Smith D. E. et al. (2010) *Space Science Reviews, 150,* 209-241. [6] Williams J. P. et al. (2019) *JGR Planets.* [7] Hayne P. O. et al. (2015) *Icarus, 255,* 58-69. [8] Mazarico E. et al. (2011) *Icarus, 211,* 1066-1081. [9] Robinson M. S. et al. (2010) *Space Science Reviews, 150,* 81-124. [10] GDAL/OGR Contributors (2019) *Open Source Geospatial Foundation.* [11] Paige D. A. et al. (2010) *Science, 330,* 479-482.

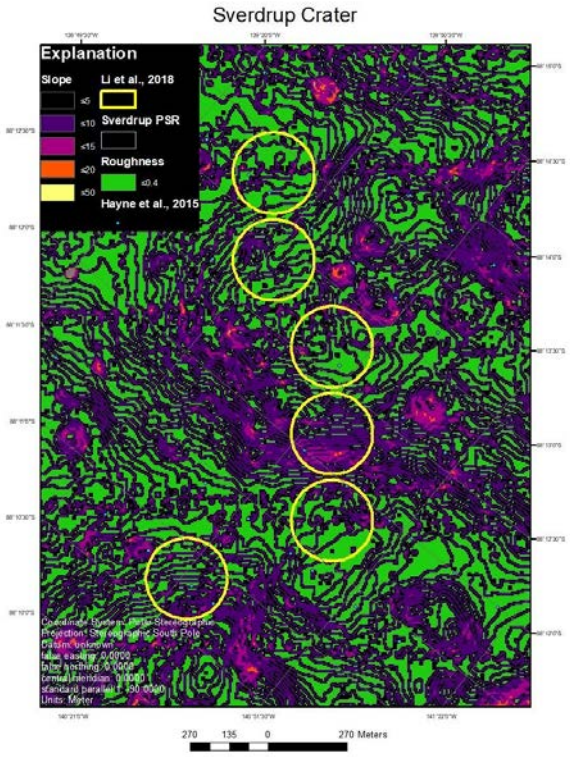

Figure 1: Top choice location for a landing site within Sverdrup crater.